Molecular Neurobiology (2019) 56:6409–6425
https://doi.org/10.1007/s12035-019-1529-y

In Vitro Priming and Hyper-Activation of Brain Microglia: an Assessment of Phenotypes

Kyle Koss[1,2] · Matthew A. Churchward[1,2] · Christopher Tsui[1,2,3] · Kathryn G. Todd[1,2,3]

Received: 27 September 2018 / Accepted: 15 February 2019 / Published online: 25 February 2019
© Springer Science+Business Media, LLC, part of Springer Nature 2019

Abstract

Microglia are the resident immune cells of the central nervous system that mediate the life and death of nervous tissue. During normal function, they exhibit a *surveying* phenotype and maintain vital functions in nervous tissue. In the event of injury or disease, chronic inflammation can result, wherein microglia develop a *hyper-activated* phenotype, shed their regenerative function, actively kill contiguous cells, and can partition injured tissue by initiating scar formation. With recoverable injury, microglia can develop a *primed* phenotype, where they appear to recover from an inflammatory event, but are limited in their support functions and show inappropriate responses to future injury often associated with neurodegenerative disorders. These microglial phenotypes were acutely recreated in vitro with potent pro- and anti-inflammatory treatments. Primary cultured microglia or mixed glia (microglia, astrocytes, and oligodendrocytes) were treated for 6 h with lipopolysaccharide (LPS). Recovery from an inflammatory state was modeled with 18-h treatment of the anti-inflammatory steroid dexamethasone. The cells were then treated for 24 h with interferon gamma (IFNγ) to detect inflammatory memory after recovery. *Surveying* was best represented in the untreated vehicle (Veh) cases and was characterized by negligible secretion of pro-inflammatory factors, limited expression of immune proteins such as induced nitric oxide synthase (iNOS), major histocompatibility complex class II (MHCII), relatively high expression of brain-derived and glial-derived neurotrophic factors (BDNF and GDNF), and thinly branched smaller microglia. *Activation* was noted in the LPS- and IFNγ-treated microglia with increased cytokines, NO, NGF, iNOS, proliferation, phagocytosis, reduced BDNF, and flattened round amoeboid-shaped microglia. *Priming* was observed to be an incomplete *surveying* restoration using dexamethasone from an *activation* comparison of LPS, IFNγ, and LPS/IFNγ. Dexamethasone treatments resulted in the most profound dysregulation of expression of NO, TNF, IL-1β, NGF, CD68, and MHCII as well as ramified morphology and uptake of myelin. These findings suggest microglial *priming* and *hyper-activation* may be effectively modeled in vitro to allow mechanistic investigations into these key cellular phenotypes.

Keywords Microglia · Phenotypes · Glia · Primed · Activated · Hyper-activated · In vitro · LPS · Interferon gamma · Dexamethasone

Introduction

Inflammatory disorders of the central nervous system (CNS), or neuroinflammatory disorders, contribute extensively to mortality and morbidity across the world. Neuroinflammation-related forms of physical and mental impairment include a broad spectrum of illnesses ranging from traumatic injury to the spinal cord and brain, stroke, and every neurodegenerative disease [1–3]. While the cause, pathology, and symptoms of these diseases are extremely diverse, they all share a core inflammatory component. CNS resident immune cells called microglia, typically responsible for mediating healthy function, sustain inflammatory cascades that exacerbate cell stress or directly facilitate the death of neighboring cells [4]. This results in the dysfunction or loss of neural circuits, producing widely varied deficits in many functions from locomotion to cognition [5]. The resulting loss of memory, cognitive capacity, and movement has a substantial impact on both healthcare costs and quality of life. Notably, no current

✉ Kathryn G. Todd
kgtodd@ualberta.ca

[1] Neurochemical Research Unit, Department of Psychiatry, University of Alberta, Edmonton, AB T6G 2G3, Canada

[2] Neuroscience and Mental Health Institute, University of Alberta, Edmonton, AB T6G 2E1, Canada

[3] Department of Biomedical Engineering, University of Alberta, Edmonton, AB T6G 2V2, Canada

treatments can cure neuroinflammatory diseases, and many suffer progressive loss of function over time.

An ideal recovery strategy should include both suppression of inflammation and promoting rescue and regeneration of lost neural tissue. Some therapeutics, such as the corticosteroid dexamethasone, have been shown capable of attenuating inflammation and promoting neuroprotection [6–8]. Comprehensive reviews are available on the drugs and the effects on microglia in neurodegenerative disorders and CNS injury [9, 10]. Despite short-term efficacy, corticosteroids are associated with long-term adverse side effects including depression, diabetes mellitus, and even compromised immune function [6, 11] limiting their utility in the resolution of neuroinflammatory disorders.

Inflammation is a complex tissue response to pathogen and damage stimuli responsible for protection, clearance of damaged cells, and tissue healing [12]. In healthy neural tissue, the blood-brain barrier (BBB) prevents trafficking of peripheral immune cells [13]. As such, the CNS has a specialized resident immune system that comprises one known major cell type, namely microglia [14]. Microglia have classic immune functions comparable to macrophages outside the CNS and are functionally similar in their response to pathogens and damaging stimuli. Microglia can be induced to M1- and M2-like phenotypes in vitro, which correlate with pro-inflammatory and anti-inflammatory macrophage activation, respectively [15, 16]. However, these labels are being shown to be less accurate in microglia due to specialization resulting from their intimate relationship with neural and glial cells within the CNS parenchyma, their isolation from circulating immune cells, and an in vitro model that does not closely reflect expected neurophysiology [15]. Thus, microglia have acquired multiple diverse functional roles which can be represented as several phenotypes across a spectrum of behaviour (Fig. 1) [17].

In the absence of harmful stimuli, microglia present a *surveying* phenotype and are essential in development, plasticity, and function of the nervous system. *Surveying* microglia secrete brain and glial-derived neurotrophic factors (BDNF, GDNF) and nerve growth factors (NGF) to promote cellular differentiation, facilitate dendritic budding and synaptic pruning to refine neuronal networks, and rapidly traverse and survey the environment [18]. They also secrete anti-inflammatory cytokines, such as interleukin 10 (IL-10), to signal other microglia to maintain the surveillant state [19–21]. They exhibit a characteristic ramified morphology, which allows them to rapidly extend multiple processes and survey the equilibrium of the resident micro-environment [22].

When exposed to a harmful stimulus, microglia present an *activated* or *reactive* phenotype that retracts processes, appearing amoeboid. Activated microglia secrete an abundance of reactive oxygen/nitrogen species such as nitric oxide (NO) produced by inducible nitric oxide synthase (iNOS), and pro-inflammatory cytokines such as tumor necrosis factor (TNF) and interleukin 1 beta (IL-1β) to recruit immune cells and kill foreign or damaged cells (e.g., pathogens, injured neurons, cancer, etc.) [23]. In the activated state, microglia will also phagocytose debris, present antigens, and incite a host response. If unresolved, inflammation becomes chronic and this *activated* phenotype can become amplified and persistent, called *hyper-activated*, causing further degradation of tissue and weakening the BBB [17].

The recovery of *activated* microglia to the *surveying* state is considered the normal functional outcome following resolution of inflammation; however, a *primed* phenotype has been proposed in the case of partial or incomplete resolution of injury. These cells may provide a means of immune memory or serve to translate repetitive mild injury into an escalating inflammatory response, and may play key roles in chronic inflammation and neurodegenerative complications including progressive white matter reduction, auto-immunity, and cognitive decline in dementia [24–29]. This *primed* phenotype has been observed to appear morphologically comparable to the surveying state but may be deficient in homeostatic and surveillance functions (often considered similar to cellular senescence) [26, 30]. Importantly, the primed state is thought to give rise to either a disproportionate or ineffectual inflammatory response upon presentation of a subsequent immune stimulus. *Hyper-activated* microglia also recruit and activate astrocytes to a secondary immune role, reducing their normal capacity to support and maintain neurons [24]. Once activated, astrocytes also undergo a phenotypical change and a process called astrogliosis, noted by cellular hypertrophy and upregulation of glial fibrillary acidic protein (GFAP). With focal injuries, such as traumatic brain and spinal cord injuries or lesions in Parkinson's disease, astrogliosis results in the formation of a glial scar intended to protect adjacent tissue from further damage; however, such scarring ultimately prevents axonal regeneration and full recovery [31–33]. Oligodendrocytes, responsible for myelinating axons in white matter, are also highly sensitive to damage by microglia in their *hyper-activated* state and are readily phagocytosed when injured [24, 34]. The presence of *primed* and *hyper-activated* microglia in effectively every neuroinflammatory disorder highlights their contribution to disease pathology, but also makes them key targets for therapy [35–43].

Although mechanisms of microglial activation have been well characterized through in vitro work, mechanisms associated with the *priming* phenotype are rather underexplored, and no effective in vitro model has been established to characterize these changes. In the present study, a series of defined treatments has been used to recreate a model of *hyper-activated* and *primed* microglial phenotypes in vitro. Microglia, in both isolated cultures and mixed glial cultures (microglia, astrocytes, and oligodendrocytes), were treated with lipopolysaccharide (LPS) [44], recovery was modeled with the anti-

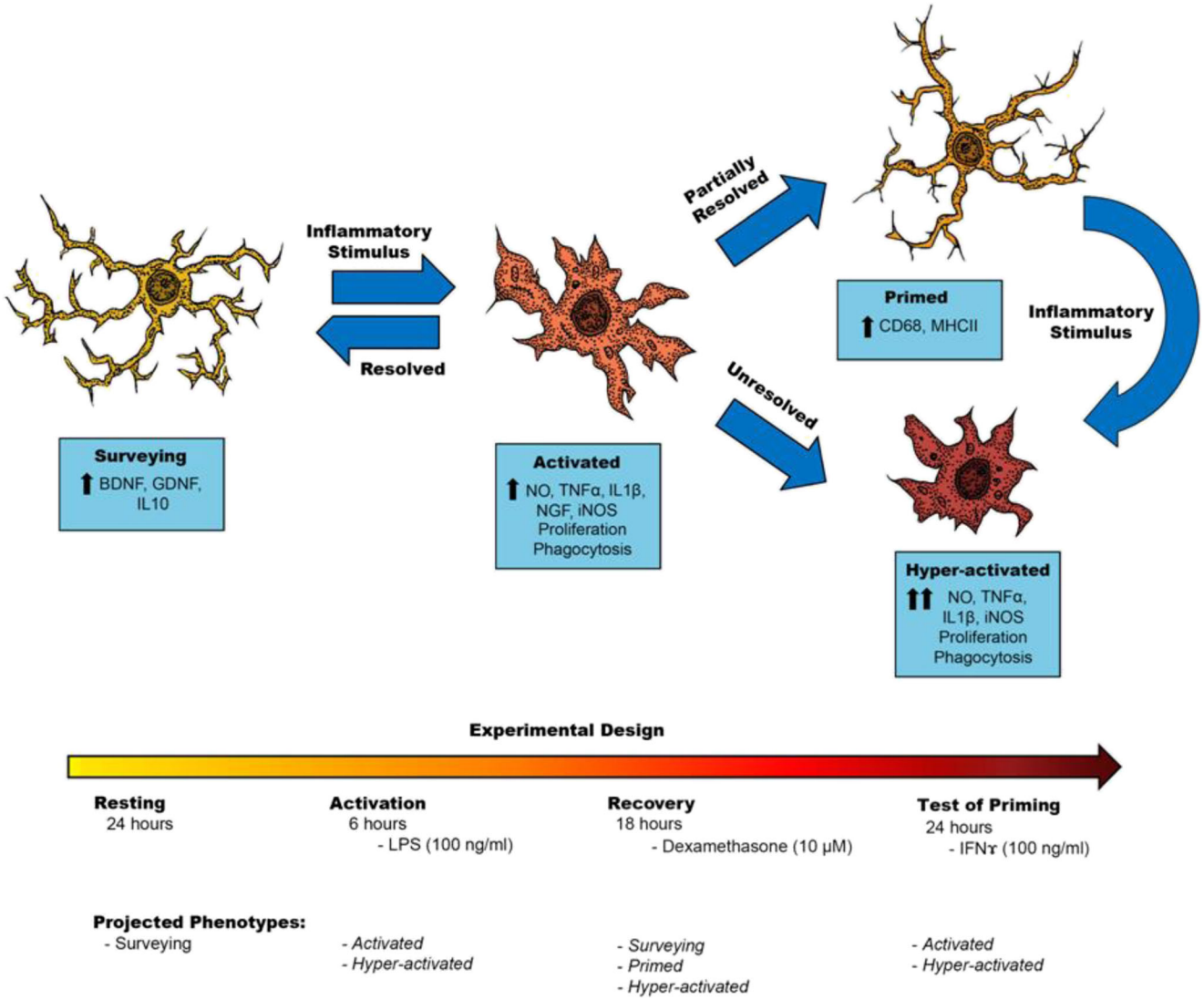

Fig. 1 The phenotypes of microglia in states of neuroinflammation. *Surveying* microglia secrete anti-inflammatory cytokines (IL10) and neurotrophic growth factors (BDNF, GDNF). Microglia are *activated* by an acute insult and respond with cytokine, chemokine, NGF, and superoxide secretions with an increase of membrane proteins (iNOS). Some *activated* microglia retain a *primed* profile characterized by different membrane proteins (MHCII, CD68). *Activated* or *primed* cells can have a persistent chronic stimulation making them *hyper-activated*—meaning they can have an amplified *activated* profile. *Primed* microglia do not fully resolve from the inflammatory insult. Adapted from [17].

inflammatory corticosteroid dexamethasone, and memory of activation as a model of priming was assessed by subsequently challenging the cells with interferon gamma (IFNγ) [45]. Microglial function was assessed by secretion of cytokines (TNF, IL-1β, IL-10), nitric oxide (NO), and growth factors (BDNF, GDNF, NGF), immunofluorescence to determine microglial morphology and expression of state markers (iNOS, CD68, MHCII), and assays of proliferation (5-Ethynyl-2′-deoxyuridine—EdU) and phagocytosis (microbeads and myelin).

The experimental design is also presented where an untreated condition suggests a *surveying* phenotype outcome. A 6-h inflammatory stimulus (LPS) promotes either an *activated* or *hyper-activating* phenotype. A recovery for 18 h (dexamethasone) promotes either a return to a *surveying*, a *primed* phenotype, or a non recovery presented as a *hyper-activation*. An additional 24-h stimulus (IFNγ) suggests *activation* if the microglia recovered fully, or *hyper-activation* with previous *priming*.

Results

The timeline and experimental design are summarized as follows. The cells were activated by pre-treating with the inflammogen lipopolysaccharide (LPS, 100 ng/mL) for 6 h and recovered with an 18-h treatment with dexamethasone (Dex, 10 μM), a potent anti-inflammatory corticosteroid, or vehicle (Veh). Drug was washed out and these cells were

subsequently challenged with interferon gamma (IFNγ, 100 ng/mL) for 24 h to probe the immune status of the cells and test for evidence of priming by their previous activation.

Nitric oxide and the major cytokines TNF and IL-1β were measured to assess pro-inflammatory secretions while the cytokine IL-10 was measured to determine anti-inflammatory secretion from the cells (Fig. 2). Typically, cultures subject to LPS pre-treatment alone, IFNγ challenge alone, and sequential LPS and IFNγ treatment showed a characteristic increase in all pro-inflammatory factors from isolated microglial cultures. Treating microglia with dexamethasone between LPS pre-treatment and IFNγ challenge promoted a significant reduction of TNF, nitrites, and IL-1β (Fig. 2(Ai–iii)) in most activating treatments, but no significant changes in IL-10 were seen in any treatment group (Fig. 2(Aiv)). These same treatments were replicated in a mixed glia culture, consisting of astrocytes, microglia, and oligodendrocytes, in order to confirm the response in a more holistic representation of the in vivo environment capable of modeling glial cell-cell interactions. In mixed glial populations, the absolute magnitude of the response was less than in isolated populations, though similar trends were observed. Typically, pro-inflammatory stimuli increased the secretion of pro-inflammatory factors, notably IFNγ and LPS/IFNγ significantly increased NO, TNF, and IL-1β release (Fig. 2(Bi-iii)), while IL-10 secretion was notably increased following LPS/ IFNγ treatment relative to control (Fig. 2(Biv)). Six-hour LPS treatment alone did not show significant increases in NO, TNF, or IL-1β, and after IFN challenge showed lower release of TNF than IFN alone and increased release of IL-10 relative to control and IFN . This suggests the persistence of activation induced by LPS pre-treatment in mixed populations is more limited than in the isolated condition, possibly due to modulatory signaling from additional glial cell types (Fig. 2(B)). Dexamethasone treatment significantly reduced the release of NO, TNF, IL-1β, and IL-10 relative to IFNγ and LPS/IFNγ treated cells (Fig. 2(Bi–iv)), though TNF remained significantly higher than control after IFNγ and dexamethasone treatment. Although dexamethasone was generally able to reduce secretion of typical inflammatory factors, reduced release of trophic release may be suggestive of a *priming* phenotype.

Endogenous growth factors BDNF, GDNF, and NGF were measured via in-cell Western assays to assess the trophic response of microglia and mixed glia (Fig. 3). Representative examples of immunofluorescent confocal images of microglia and mixed glia are presented to demonstrate the subcellular distribution of growth factors. In isolated microglia, BDNF expression was elevated in the control groups and was significantly reduced with LPS, IFNγ, or sequential LPS/IFNγ treatment (Fig. 3(Ai)). Following treatment with dexamethasone, BDNF expression was similarly increased in the control relative to LPS, IFN , and LPS/IFN -treated cultures. Expression of GDNF was consistent within the Veh groups and did not significantly vary with LPS, IFNγ, or sequential LPS/IFNγ treatments, nor did dexamethasone treatment significantly affect GDNF secretion (Fig 3(Aii)). NGF expression significantly increased in isolated microglia in the LPS treatment group (Fig 3(Aiii)), but this pattern of increased NGF expression was not observed following dexamethasone recovery treatment, suggesting that dexamethasone recovery attenuated the potential trophic support provided by microglia. In mixed glia, expression of trophic factors was markedly less variable across the different treatments, and

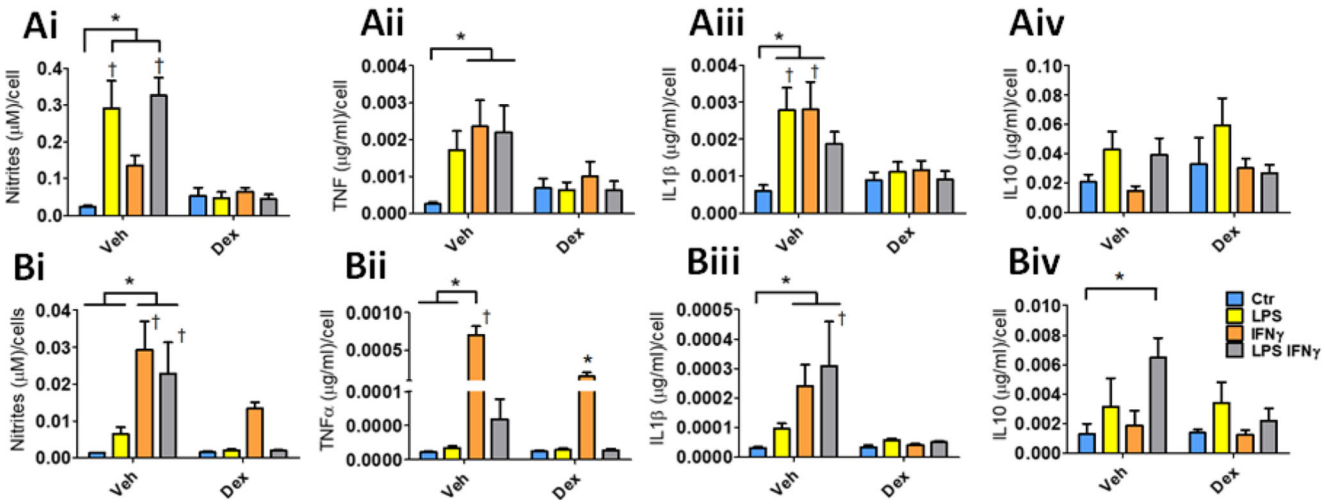

Fig. 2 Inflammatory molecular assays for primary rat (A) isolated microglia and (B) mixed glia, including (i) nitrite, and ELISA results for (ii) TNF, (iii) IL-1β, and (iv) IL-10 release normalized to cell count. Samples were treated with 100 ng/mL lipopolysaccharide (LPS) for 6 h, followed by 18 h of 10 μM dexamethasone (Dex), and a 24 h 100 ng/mL treatment with interferon gamma (IFN). $n = 5$ for all groups and data analyzed represent mean ± SEM. Significance indicated for a p value of ≤ 0.05, where * indicates within group differences as indicated, and † represent pair-wise differences between Veh and dexamethasone groups, respectively

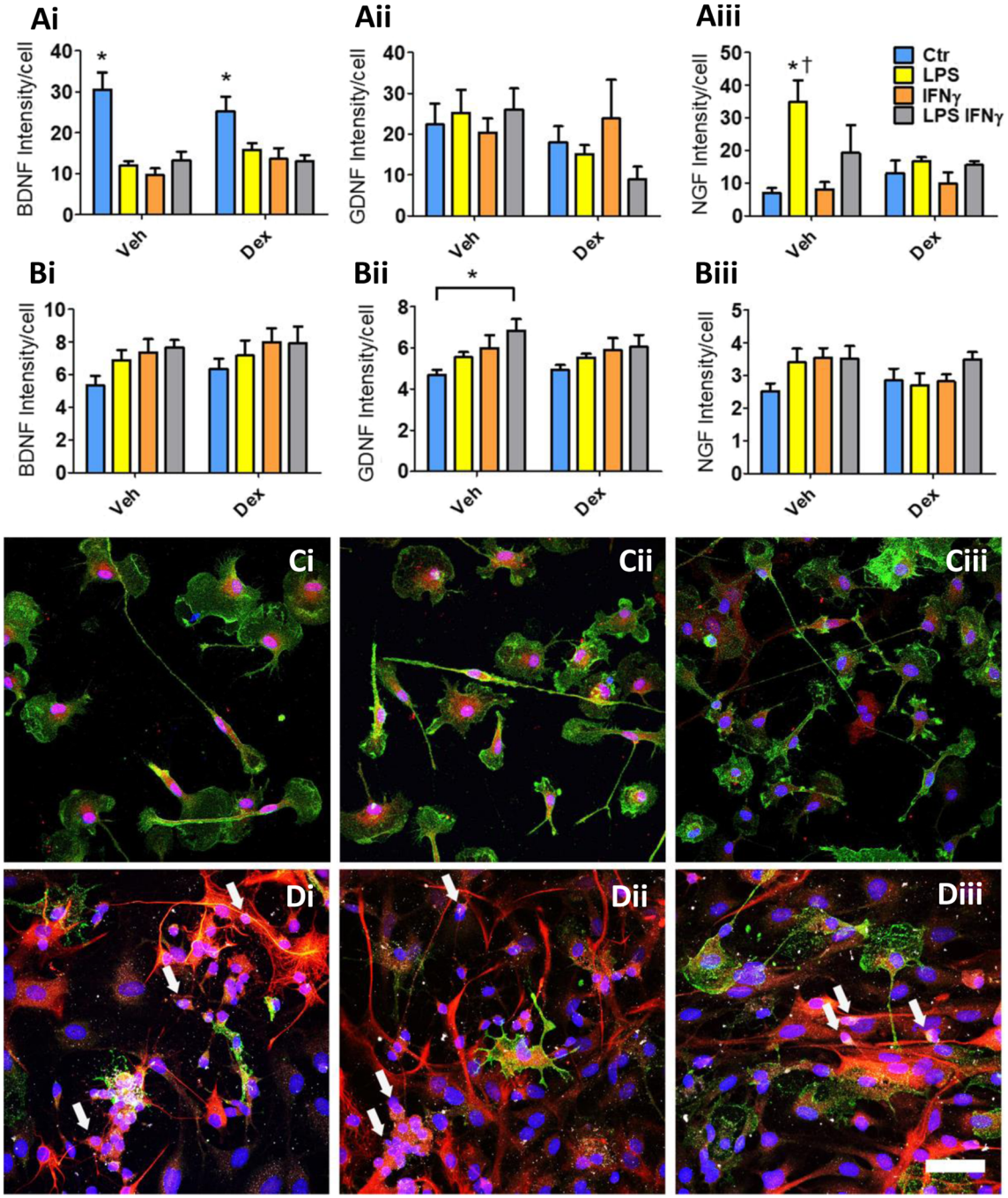

Fig. 3 In-cell Western assays to detect neurotrophic growth factors for (A) isolated microglia and (B) mixed glia, including (i) BDNF, (ii) GDNF, and (iii) NGF normalized to cell count. Samples were treated with 100 ng/mL LPS for 6 h, followed by 18 h of 10 μM dexamethasone, and a 24 h 100 ng/mL treatment with IFNγ. $n = 5$ for all groups and the data analyzed represents mean ± SEM (arbitrary fluorescence units). Significance indicated for a p value of ≤ 0.05, where * indicates within group differences as indicated, and † represent pair-wise differences between Veh and dexamethasone groups, respectively. Immunofluorescent confocal l images of (C) microglia and (D) mixed glia. Labels are as follows—Row C: blue (nuclei), green (CD11b), red (growth factor). Row D: blue (nuclei), green (CD11b), red (GFAP), white (growth factor). Arrows in D indicate cells co-labeled for GFAP and the respective growth factor. The scale bar is 50 μm

only GDNF expression was significantly increased with LPS/IFNγ compared to the control.

When observed with immunofluorescence microscopy (Fig. 3(C)), growth factor expression in isolated microglial cultures was characteristically somatic, radiating from the area surrounding the nucleus throughout the cytoplasm. Expression of both BDNF and GDNF was observed in all CD11b-labeled cells, but only a subset of cells showed NGF expression, suggesting that NGF expression may be unique to certain microglia. In a mixed glial population

(Fig. 3(D)), growth factor expression was observed less in microglia and more often in astrocytes (Fig. 3(Di–iii), white arrows). This pattern of expression suggests the relatively consistent expression of growth factors across treatment groups in mixed glia (Fig. 3(B)) was reflective of stable astrocyte expression levels overwhelming any changes in microglial expression as a result of treatment (Fig. 3(A)). The persistence of decreased BDNF expression observed in isolated microglia, even after dexamethasone recovery treatment, may suggest microglial *priming*.

As previous studies have suggested, characteristic markers of microglial function may be differentially expressed in the primed state we chose several to characterize with immunofluorescence microscopy [17, 27]. Expression of iNOS in microglia was characterized in both isolated and mixed glial populations (Fig. 4). In isolated microglia, the proportion of iNOS-positive cells was significantly increased (from ~ 5% to > 20%), compared to the control in the Veh group for all inflammatory treatments (LPS, IFNγ, and LPS/IFNγ, Fig. 4(A)). In addition, sequential treatment with LPS and IFNγ yielded substantially increased iNOS expression relative to LPS or IFNγ alone (from ~ 20 to 40%), suggesting a cumulative effect on iNOS expression. Treatment with dexamethasone prevented stimulus-induced iNOS expression in all conditions (LPS, IFNγ, and LPS/IFNγ, Fig. 4(A)). In mixed glial cultures, iNOS-positive microglia were fewer overall (~ 4 to 8%) suggesting the mixed cellular environment moderates microglial expression of iNOS in response to inflammatory stimuli. Significant differences in iNOS expression were not observed within treatment groups, and dexamethasone significantly attenuated iNOS expression by ~ 3% only in the IFNγ treatment (Veh vs Dex, Fig. 4(C)).

Cellular morphology, observed by Iba1 and iNOS co-labeling in isolated microglia, demonstrated a range of morphology (Fig. 4(B)). Isolated *surveying* microglia (control,

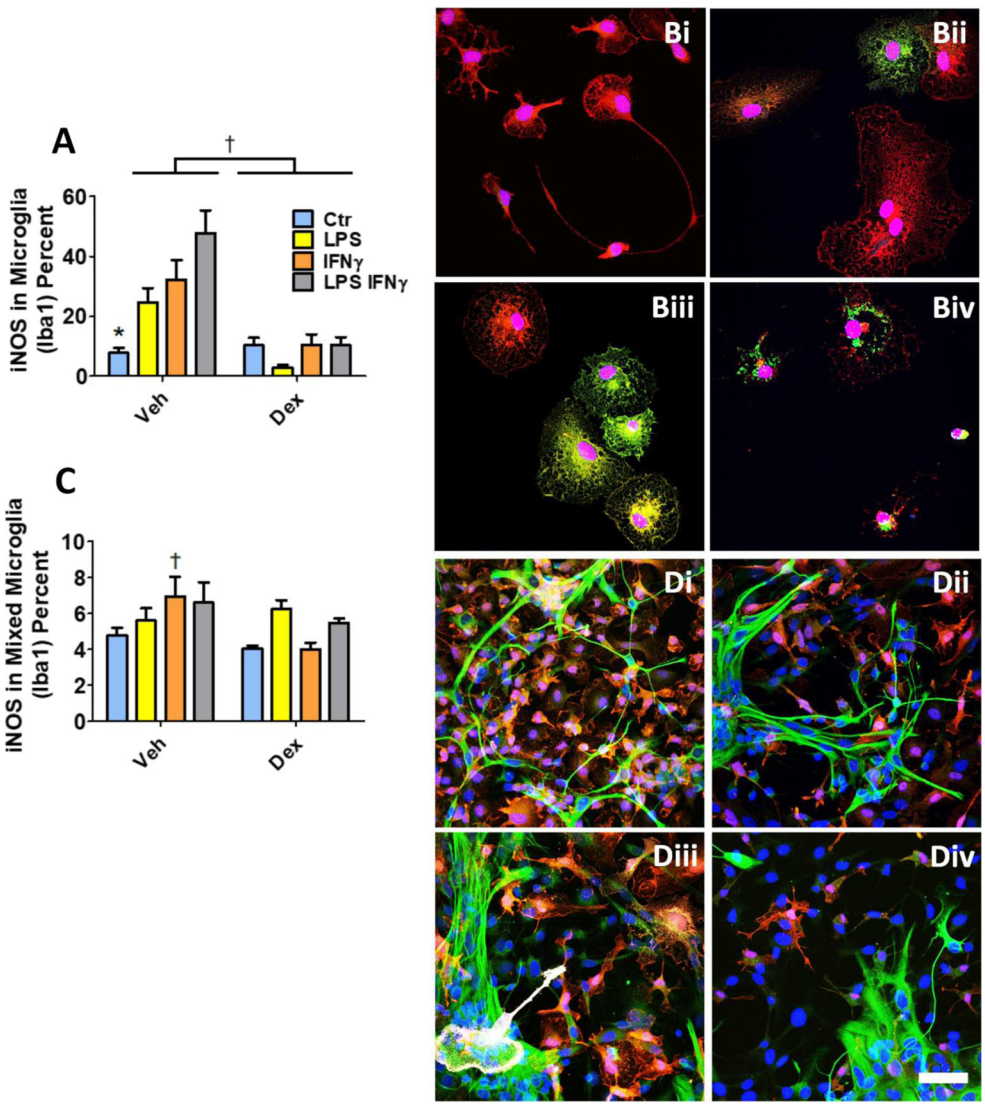

Fig. 4 Immunofluorescent quantification and confocal images of primary rat iNOS-labeled (A and B) microglia and (C and D) mixed glia. Cells were quantified by positive counts. Samples were treated with 100 ng/mL LPS for 6 h, followed by 18 h 10 μM dexamethasone, and a 24 h 100 ng/mL treatment with IFNγ. $n = 5$ for all groups and data represent mean ± SEM. Significance indicated for a p value of ≤ 0.05, where * indicates within group differences as indicated, and † represent pair-wise differences between Veh and dexamethasone groups, respectively. Confocal images present cells treated with (i) control, or (ii) LPS, (iii) LPS/IFNγ, and (iv) LPS/dexamethasone. Labels are as follows—section B: blue (nuclei), red (Iba1), green (iNOS). Section D: blue (nuclei), red (Iba1), green (GFAP), white (iNOS). The scale bar is 50 μm

Fig 4(Bi)) had multiple thin and bifurcated processes with no visible iNOS expression, while microglia treated with pro-inflammatory stimuli (LPS and LPS/IFNγ, Fig 4(Bii-iii)) appeared distinctly amoeboid with round and flattened cells showing heterogeneous iNOS expression throughout the cell cytoplasm. LPS treatment followed by dexamethasone treatment (Fig 4(Biv)) did not restore a ramified morphology, and remained notably amoeboid in appearance. Following dexamethasone treatment, iNOS was observed but was less broadly dispersed through the volume of the cell. In the mixed glial cultures, the morphological features observed in isolated cells tended to be less exaggerated with microglial cells rarely expressing iNOS (Fig. 4(D)). *Surveying* microglia in the control group (Fig 4(Di)) were morphologically similar to the isolated condition with elongated processes. Microglia treated with pro-inflammatory stimuli (LPS and IFNγ/LPS, Fig 4(Dii, iii)) were less amoeboid than in the isolated culture and retained a ramified morphology following LPS/dexamethasone treatment (Fig 4(Div)). Although GFAP-positive astrocytes tended to lose their thin processes and radial microstructures to favor a hypertrophic and/or fibrous morphology after LPS and IFNγ/LPS treatment, the distribution of cells appears diverse in each treatment. iNOS expression generally correlated closely with NO secretion (Fig. 2) and was suggestive of *activation* and *hyper-active* microglia.

CD68, a lysosomal microglial glycoprotein, is characteristically upregulated for a prolonged period after pro-inflammatory stimulus and has been suggested to associate with *priming* in vivo [17]. In isolated microglia cultures, CD68 was notably high in the control condition, and decreased significantly from control following treatment with either LPS or IFNγ/LPS (Fig. 5(A)). Dexamethasone treatment significantly increased CD68 expression in all stimulated conditions (LPS, IFNγ, and LPS/IFNγ treatment, Veh vs Dex). As CD68 is hypothesized to increase with *priming*, these results suggest a primed state was induced following dexamethasone treatment.

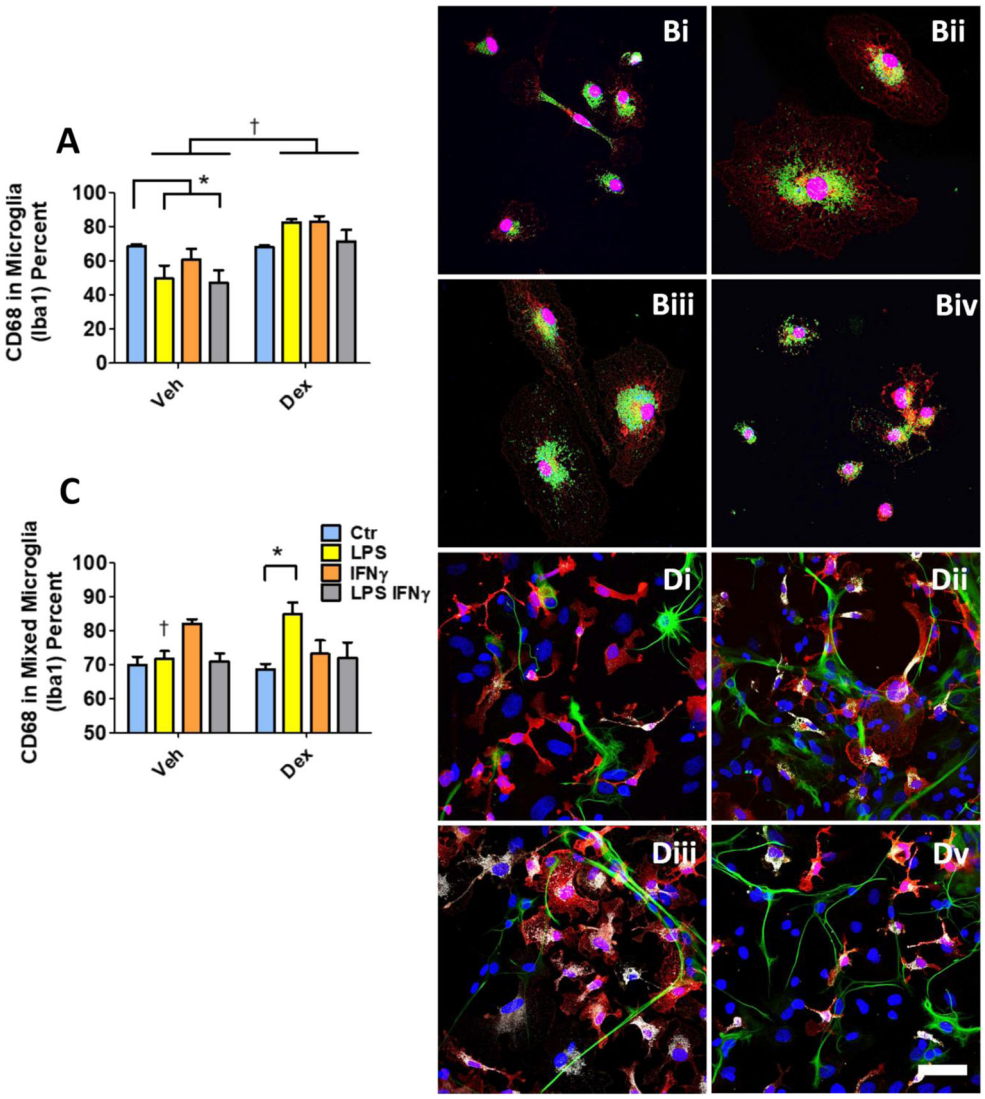

Fig. 5 Immunofluorescent quantification and confocal images of primary rat CD68-labeled (A and B) microglia and (C and D) mixed glia. Cells were quantified by positive counts. Samples were treated with 100 ng/mL LPS for 6 h, followed by 18 h of 10 μM dexamethasone, and a 24 h 100 ng/mL treatment with IFNγ. $n = 5$ for all groups and data represent mean ± SEM. Significance indicated for a p value of ≤ 0.05, where * indicates within group differences as indicated, and † represent pair-wise differences between Veh and dexamethasone groups, respectively. Confocal images present cells treated with (i) control, or (ii) LPS, (iii) LPS retreated with IFNγ, and (iv) LPS recovered with dexamethasone. Labels are as follows—section B: blue (nuclei), red (Iba1), green (CD68). Section D: blue (nuclei), red (Iba1), green (GFAP), white (CD68). The scale bar is 50 μm

In mixed glial cultures, a significant increase in CD68-positive microglia was only observed following IFNγ treatment, but this expression was decreased after dexamethasone recovery (Fig. 5(C)). Curiously, microglia treated with LPS prior to dexamethasone treatment showed a significantly higher proportion of CD68 expression as compared to the control, suggesting dexamethasone treatment may have prevented recovery of CD68 levels to that of control and possibly indicating persistence of activation (Fig. 5(C)). Morphologically, CD68 expression in microglia was observed in a characteristic punctate pattern, consistent with lysosomal localization, typically favoring the cell soma with limited labelling into projections and was prevalent in a large proportion of cells (Fig. 5(B, D)).

MHCII is a membrane-bound protein complex associated with antigen presentation and immune memory. In isolated microglia, MHCII expression was negligible in the control groups while the proportion of MHCII-positive cells was significantly increased after LPS, IFNγ and LPS/IFNγ treatments (Fig. 6(A)). Treatment with dexamethasone prevented any significant increase in MHCII expression in LPS, IFNγ, and LPS/IFNγ-treated cells (relative to dexamethasone treated control condition, Fig. 6(A)). Notably, MHCII expression was significantly lower in the dexamethasone/IFNγ condition than in the Veh/IFNγ condition. MHCII expression in microglia within mixed glial cultures followed a comparable pattern, and was significantly higher than the within group control in both the IFNγ-treated and dexamethasone/IFNγ-treated groups; however, dexamethasone treatment significantly decreased MHCII expression in the IFNγ treatment group (Veh vs Dex, Fig. 6(C)). Fluorescence microscopy showed distinct MHCII expression either within the cell soma (Fig. 6(B, D)) or continuously through the cell cytoplasm (Fig 6(Dii)). In both isolated cultures and mixed glial cultures, MHCII-positive microglia were highest in IFNγ (up to 50%), but were reduced to approximately 20–30% by prior LPS exposure. Although increased MHCII expression is proposed to follow *priming*, within our experiments expression did not increase with sequential activating stimuli. It is possible that MHCII as a marker of *priming* is dependent on the nature of the initial stimulus, as pre-treatment with LPS, a pathogenic stimulus, consistently lead to a decreased expression of MHCII after IFNγ challenge.

Secretory profiles and marker expression microglia are common and useful descriptors of an activated phenotype; however, functional metrics such as increased microglial phagocytosis and proliferation are important features of activation. Thus, we sought to assess these functional outputs in relation to the induced microglial phenotypes. Proliferation was assessed by incorporation of the synthetic nucleotide EdU, visualized using immunofluorescence microscopy, and quantified for Iba1-positive microglia in isolated and mixed glia cultures (Fig. 7). In isolated microglia cultures, proliferation (EdU-positive cells) significantly increased in both the LPS and LPS/IFNγ treatment groups. Dexamethasone treatment prevented an increase in the proportion of EdU-positive cells in both LPS and LPS/IFNγ, suggesting that proliferation was attenuated by this drug. In mixed glial cultures, EdU incorporation in microglia (co-labeled with Iba1) increased significantly in both the IFNγ and LPS/IFNγ groups, and as with isolated microglia, dexamethasone recovery treatment significantly reduced proliferation in both groups.

Phagocytosis was assessed by measuring uptake of green fluorescent polystyrene microbeads in isolated microglia, and was quantified as both the percent of cells taking up at least one bead (Fig. 8Ai, Aiii) and the mean uptake (integrated fluorescence) per cell taking up at least one bead (Fig. 8Aii). In addition, microbead uptake in isolated microglia cultures was characterized in subcategories based on iNOS, CD68, and MHCII expression. In isolated microglia cultures, all activating treatments (LPS, IFNγ, and LPS/IFNγ) significantly increased the percentage of cells taking up beads relative to control, and this effect was attenuated by dexamethasone treatment (Fig. 8Ai). When assessing average uptake per cell, isolated microglia internalized significantly more beads with both LPS and LPS/IFNγ treatments, and again this effect was prevented by dexamethasone treatment (Fig. 8(Aii)). In mixed glia, phagocytic activity was determined by measuring microglial uptake of myelin debris using CNPase immunofluorescence (Fig 8(Bi–iii)). Iba1-positive microglia with CNPase debris significantly increased with all activating groups (LPS, IFNγ, LPS/IFNγ) relative to control, and this effect was significantly attenuated following dexamethasone recovery treatment. As with microbead uptake in isolated microglia, CNPase accumulation per cell was significantly higher in cultures treated with LPS (both LPS and LPS/IFNγ groups), and this was significantly reduced by dexamethasone treatment in the LPS group. Microglia treated with LPS, dexamethasone, and IFNγ had significantly more CNPase material per cell than the respective control and was not significantly different than the vehicle, LPS/IFNγ group.

Within isolated cultures, most iNOS and MHCII-positive microglia took up microbeads, with insignificant variation between treatments (Fig 8(Ci, v)); however, CD68-positive cells closely mirrored the population average for all Iba1-positive cells (Fig 8(Ciii)). Considering that most microglia were bead-positive (Fig. 8(Ai)), it is reasonable to expect microbeads in these labeled cells. However, total uptake of microbeads per cell was notably different in the iNOS group (Fig 8(Cii)). iNOS expressing microglia in the control condition had markedly higher total microbead uptake relative to all LPS, IFNγ, and LPS/IFNγ treatments. In addition, dexamethasone recovery treatment was able to significantly reduce the quantity of internalized beads in the control group, but not in any other

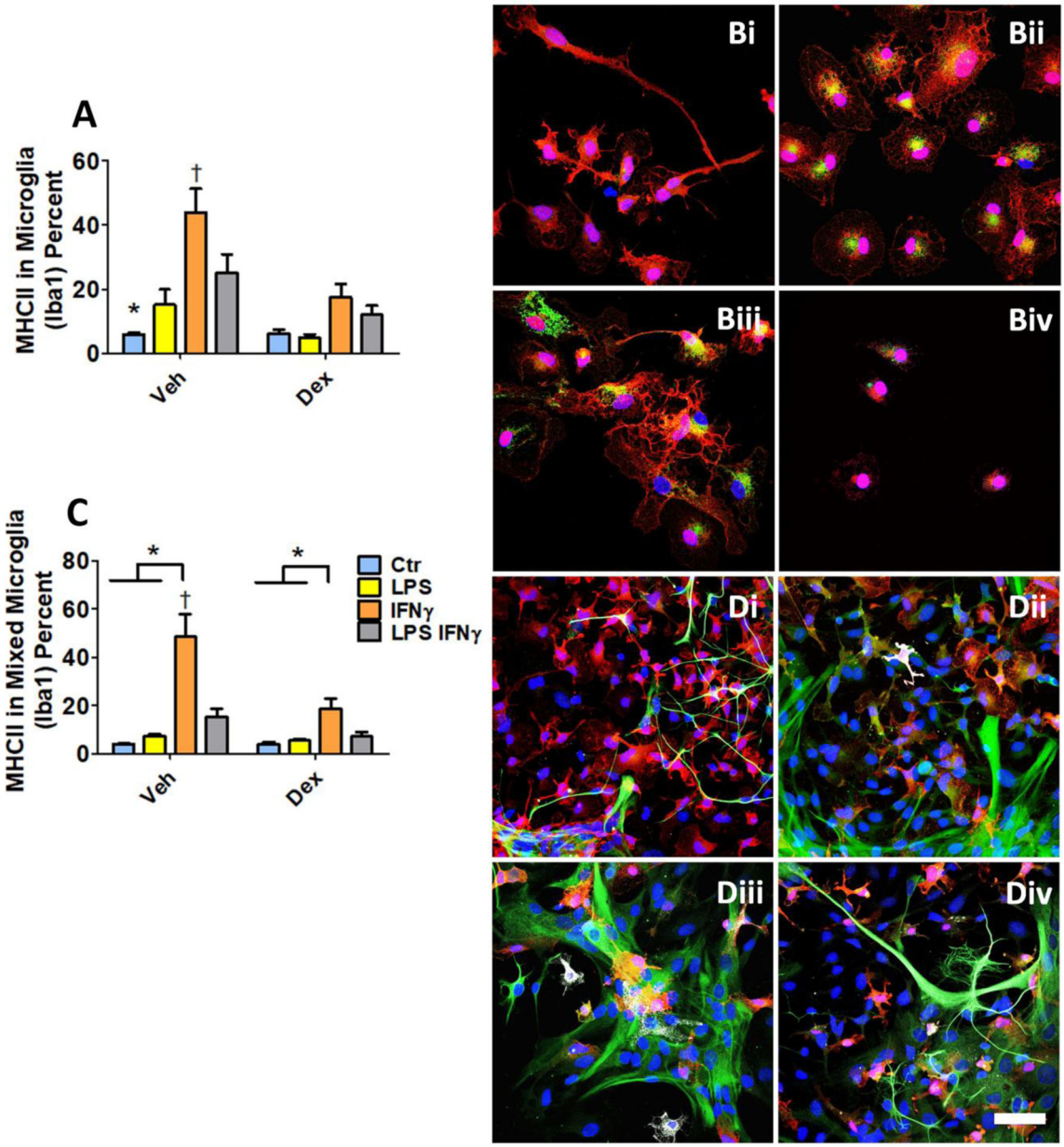

Fig. 6 Immunofluorescent quantification and confocal images of primary rat MHCII-labeled (A and B) microglia and (C and D) mixed glia. Cells were quantified by positive counts. Samples were treated with 100 ng/mL LPS for 6 h, followed by 18 h of 10 μM dexamethasone, and a 24 h 100 ng/mL treatment with IFNγ. $n = 5$ for all groups and data represent mean ± SEM. Significance indicated for a p value of ≤ 0.05, where * indicates within group differences as indicated, and † represent pairwise differences between Veh and dexamethasone groups, respectively. Confocal images present cells treated with (i) control, or (ii) LPS, (iii) LPS retreated with IFNγ, and (iv) LPS recovered with dexamethasone. Labels are as follows—section B: blue (nuclei), red (Iba1), green (MHCII). Section D: blue (nuclei), red (Iba1), green (GFAP), white (MHCII). The scale bar is 50 μm

groups. As stated previously, in the control group, iNOS-expressing cells were few (< 10%) and as such the function of this subpopulation is unclear. Bead uptake per cell in both CD68 and MHCII expressing microglia (Fig 8(Civ, vi)) closely resembled the population average (Fig 8(Aii)). Significant increases in bead uptake were observed for both LPS and LPS/IFNγ groups, and this increase was attenuated by dexamethasone recovery treatment.

Discussion

Through the course of the above activations and recovery treatments, several microglial phenotypes were observed that may correlate with phenotypes described in vivo (Tables 1 and 2). As expected, in this model, the untreated control group may best represent the ramified, or *surveying*, phenotype. This is exemplified by low secretion of pro-inflammatory

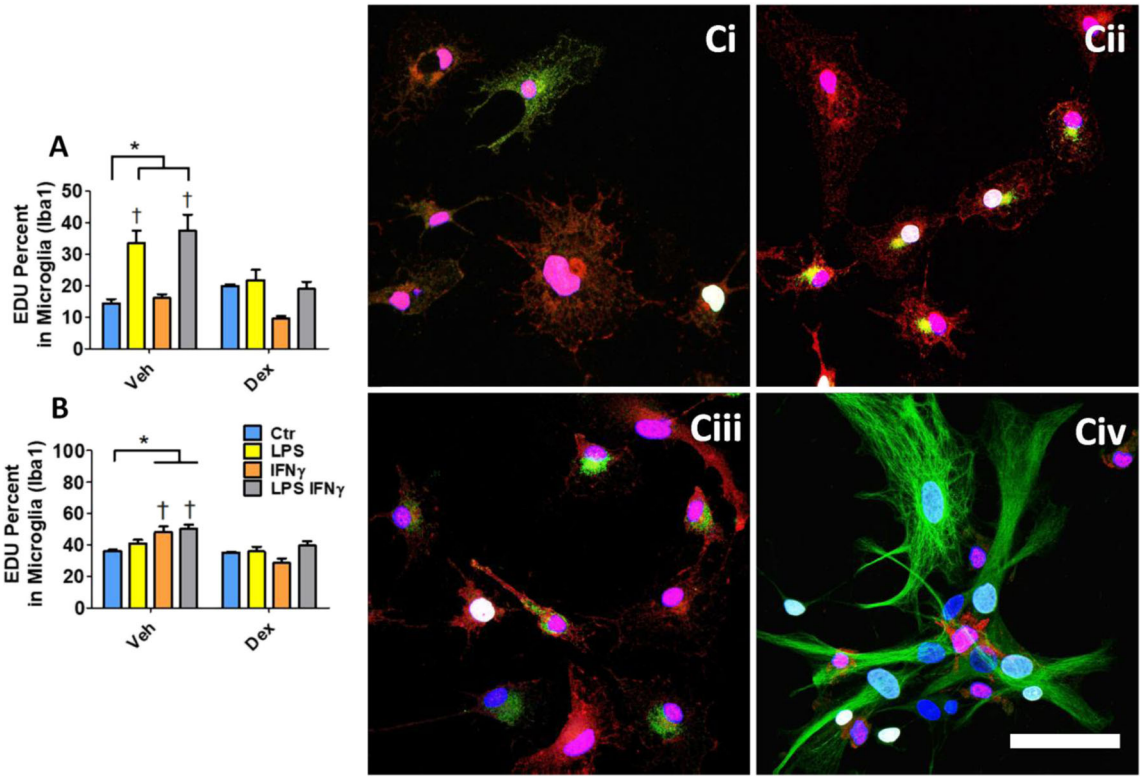

Fig. 7 Immunofluorescent quantification of EdU labelling in (A) isolated microglia, (B) mixed population microglia, and (C) representative confocal images. Cells were quantified by positive counts. Samples were treated with 100 ng/mL LPS for 6 h, followed by 18 h of 10 μM dexamethasone, and a 24 h 100 ng/mL treatment with IFNγ. $n = 5$ for all groups and data represents mean ± SEM. Significance indicated for a p value of ≤ 0.05, where * indicates within group differences as indicated, and † represent pair-wise differences between Veh and dexamethasone groups, respectively. Confocal image labels are Iba1 in red for microglia, (i) iNOS, (ii) CD68, (iii) MHCII, and (iv) GFAP (astrocytes) in green, EdU in white, and Hoescht blue for nuclei. The scale bar is 50 μm

cytokines and NO, minimal iNOS and MHCII expression, high BDNF and GDNF expression, and morphologically smaller cell bodies with thin branching processes. In addition, microglial proliferation and phagocytosis are generally lower in *surveying* microglia. These effects are expected (Fig. 1) and have been noted in the majority of the literature [18, 46–48]. With the exception BDNF expression, most effects were consistently observed in both isolated microglia cultures and mixed glial populations.

Activation is characterized by increased cytokines, NO, iNOS, phagocytosis, and proliferation, while BDNF and GDNF are reduced [49–51]. Microglia morphology transforms into a flattened round shape. Interestingly, anti-inflammatory IL-10 (Fig 2(Biv)), GDNF (Fig. 3(Bii)), and NGF (Fig. 3(Aiii)) levels increased with LPS and LPS/IFNγ treatments, suggesting a trophic response during activation which has been noted in other studies [20, 52]. MHCII expression also mirrored iNOS expression across groups and was far more pronounced than iNOS in mixed microglia. This may be due to the timing of iNOS expression, measured at a fixed 24-h experimental endpoint, compared to NO levels that reflected cumulative release over 24 h of release. In addition, MHCII may have a longer-lasting expression in the cells due to the proposed role of MHCII in immune memory [14]. Distinguishing microglial *activation* vs *hyper-activation* in the course of our experimental manipulations is challenging; however, sequential treatment of isolated microglia with LPS and IFNγ produced comparable release of pro-inflammatory factors to LPS treatment alone, decreased release of NGF, and increased expression of iNOS relative to LPS treatment alone. These differences, along with the highly proliferative and phagocytic phenotype observed, suggests that sequential LPS/IFNγ treatment may represent *hyperactivity* compared to LPS treatment alone, though further experimentation may be required to elicit a broadly exaggerated inflammatory phenotype. Dexamethasone had a pronounced treatment effect across most of the dependent variables assessed as it reduced levels of NO, TNF, IL-1β, and expression of MHCII and iNOS to the control (*surveying*) baseline. This is unsurprising considering that dexamethasone is a very potent anti-inflammatory molecule; however, dexamethasone is not often considered a neuroprotective treatment [53–56], as we observed in the mixed effects of dexamethasone treatment on anti-inflammatory cytokine IL-10 (Fig. 2(Aiv, Biv)) and growth factors BDNF, GDNF, and NGF (Fig. 3). Given that LPS is considered a potent activator and the 6-h treatment course represents an accepted timeline to activate microglia

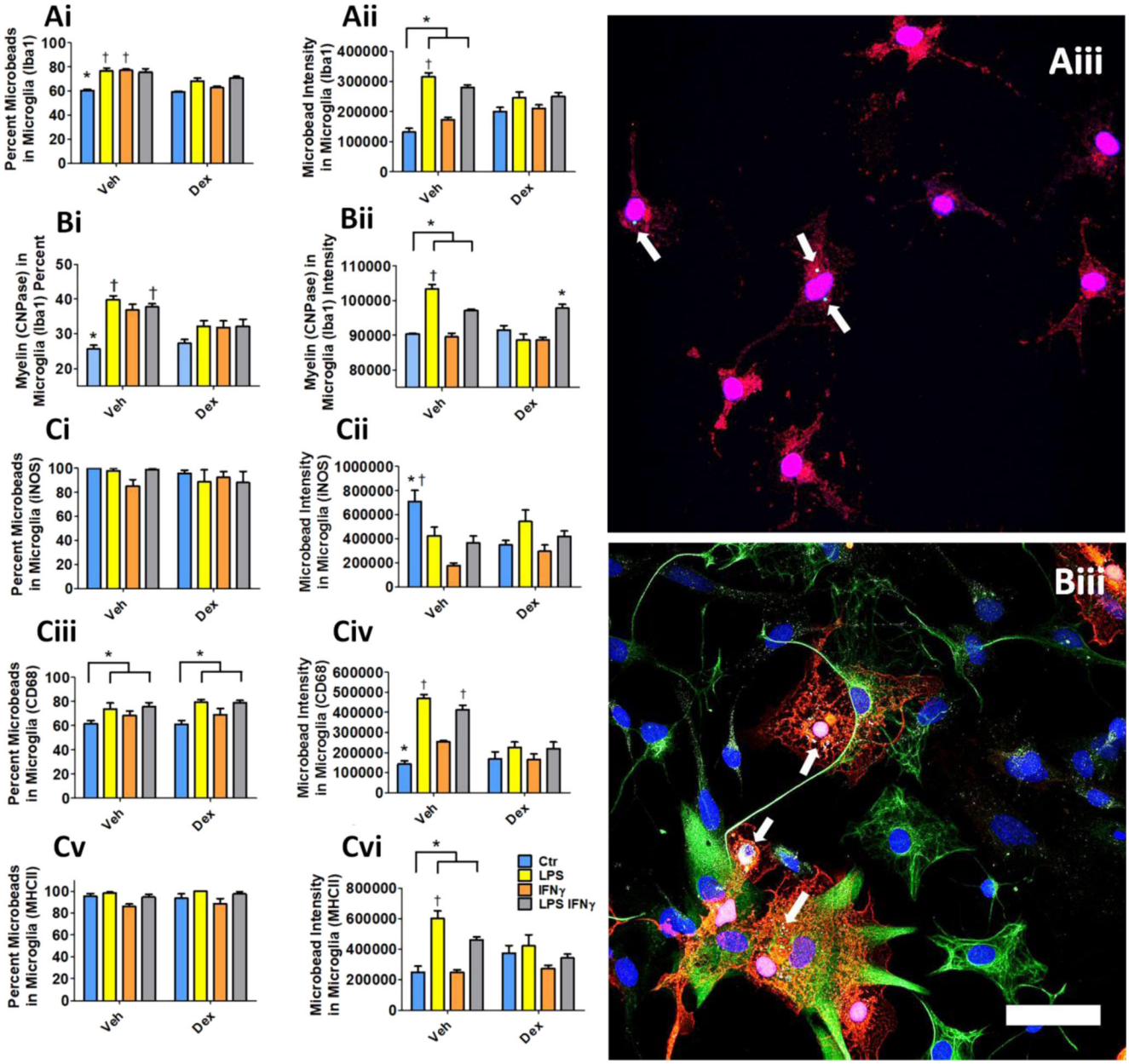

Fig. 8 Immunofluorescent quantification of phagocytosis labelling in (A) isolated microglial microbead uptake, (B) microglial CNPase (myelin) uptake in mixed glia, (C) isolated microglial microbead uptake in (i, ii) iNOS, (iii, iv) CD68, and (v, vi) MHCII-positive microglia. Samples were treated with 100 ng/mL LPS for 6 h, followed by 18 h of 10 μM dexamethasone, and a 24 h 100 ng/mL treatment with IFNγ. $n = 5$ for all groups and data represent mean ± SEM. Significance indicated for a p value of ≤ 0.05, where * indicates within group differences as indicated, and † represent pair-wise differences between Veh and dexamethasone groups, respectively. Cells were quantified by positive counts and average counted intensity. Representative (iii) confocal image labels are Iba1 in red for microglia, (A) microbeads, and (B) CNPase for oligodendrocytes/myelin in white, GFAP in green for astrocytes, and Hoescht blue for nuclei. Arrows indicate uptake of beads (Aiii) or myelin (Biii) into microglia The scale bar is 50 μm

and macrophages [57–61], future work may warrant sequential or sustained treatment with LPS for longer time periods.

To assess the nature of microglial *priming* after recovery treatment, we challenged LPS pre-treated cells with IFNγ after an 18-h rest period (with or without dexamethasone treatment). Based on previous reports, increased CD68 and MHCII expression were expected indicators of this phenotype [17]. Absent any recovery treatment, IFNγ challenge resulted in elevated levels of iNOS and MHCII relative to the LPS pre-treatment group (Figs. 4 and 6) while sustained release of pro-inflammatory cytokines, NO, and expression of CD68 were observed (Figs. 2 and 5). Dexamethasone treatment generally suppressed cytokine release to comparable levels to control (Fig. 2); however, following dexamethasone washout, a subsequent IFNγ challenge failed to induce secretion of pro-inflammatory cytokines, NO, or IL-10, and comparable effects

Table 1 Summary of treatment effects on isolated microglia cultures

	Nitrite	TNF	IL-1β	IL-10	BDNF	GDNF	NGF	iNOS	CD68	MHCII	EdU	Phagocytosis (%)	Bead uptake
Control	○	○	○	○	++	+	○	○	+	○	○	+	+
LPS	++	+	++	○	–	+	++	+	–	+	+	++	++
IFNγ	+	+	++	○	–	+	○	+	+	++	○	++	+
LPS + IFNγ	++	+	+	○	–	+	+	+	–	+	+	++	++
Dexamethasone	○	○	○	○	+	+	○	○	+	○	○	+	+
LPS	○	○	○	○	–	+	○	○	+	○	○	+	+
IFNγ	○	○	○	○	–	+	○	○	+	○	○	+	+
LPS + IFNγ	○	○	○	○	–	+	○	○	+	○	○	+	+

○ Indicates negligible or low level of indicated factor measured

– Indicates decreased levels of indicated factor measured relative to the within group control

+ Indicates measurable levels of indicated factor or increased levels relative to within group control

++ Indicates high levels of indicated factor measured relative to within group control

were seen on expression of growth factors. Changes in CD68 and MHCII may relate to lysosomal activity and immune-mediated endocytosis in microglia and macrophages, which can be highly interrelated [62]. Dexamethasone treatment resulted in sustained elevation of CD68 expression (Fig. 5), which may indicate microglial *priming*; however, comparable effects were not seen on MHCII expression. This collective molecular profile may be more consistent with evidence of microglial priming resulting in dysfunction rather than hyperfunction, as has been associated with models of Parkinson's disease [63]. In addition, isolated microglia were more readily *primed* than microglia in mixed glial populations which is likely due to signaling and support from other glial cells, notably astrocyte-mediated protection [64, 65]. It is worth noting that the absolute differences in the release profile of isolated microglia and mixed glial cultures (Fig. 2) is at least partially influenced by the correction introduced into our calculations to account for differences in total cell counts. Since isolated microglia cultures are ≥95% microglia, the reported values per cell are proportionate to the number of microglia in culture, but the same correction applied to mixed glial cultures is proportionate to the total mixed population (including astrocytes and oligodendrocytes) and as such is markedly lower.

Similarly, other dependent outputs could be considered to represent *priming* when noting differences in response to LPS, IFNγ, and sequential treatment with LPS and IFNγ. Notably, pro-inflammatory release (NO, TNF, and IL-1β) was consistently higher in IFNγ than the LPS/IFNγ group (Fig. 2). This may suggest that the cells have diminished secretory capacity when responding to sequential activation stimuli. Reactive oxygen species and IL-1β have been linked to *primed* microglia in brain-related chronic stress and aging [66, 67]. In isolated microglia, a similar observation is visible with NGF expression where the IFNγ challenge demonstrated reduced

Table 2 Summary of treatment effects on mixed glia cultures

	Nitrite	TNF	IL-1β	IL-10	BDNF	GDNF	NGF	iNOS	CD68	MHCII	EdU	Phagocytosis (%)	Myelin uptake
Control	○	○	○	○	+	+	+	○	+	○	○	○	○
LPS	○	○	○	○	+	+	+	○	+	○	○	+	+
IFNγ	++	++	+	○	+	+	+	+	++	++	+	+	○
LPS + IFNγ	++	+	+	+	+	++	+	○	+	○	+	+	+
Dexamethasone	○	○	○	○	+	+	+	○	+	○	○	○	○
LPS	○	○	○	○	+	+	+	○	++	○	○	○	○
IFNγ	+	++	○	○	+	+	+	○	+	+	○	○	○
LPS + IFNγ	○	○	○	○	+	+	+	○	+	○	○	○	+

○ Indicates negligible or low level of indicated factor measured

– Indicates decreased levels of indicated factor measured relative to the within group control

+ Indicates measurable levels of indicated factor or increased levels relative to within group control

++ Indicates high levels of indicated factor measured relative to within group control

growth factor secretion [52, 68]. The loss of NGF and IL-10 trophic response may also be linked to *priming* as this state has been proposed to correlate with decreased neuroprotective microglial functions [69]. In isolated microglial cultures, iNOS expression was highest in the LPS/IFNγ group compared to the other treatments. Cellular morphology cannot be used alone to determine activation state; however, when coupled with the measured release and expression profile can inform our evaluations. In both isolated microglia and mixed glial cultures, dexamethasone-treated microglia lost their amoeboid shapes and appeared smaller but with fewer ramifications than the control condition. This suggests a microglial phenotype that may not be acutely activated but has not returned to a surveying phenotype typical of the ramified morphology. Microglia have been demonstrated to transition between different morphologies readily in vivo; however, with the more limited time course of in vitro experiments, treatment with dexamethasone was required to witness changes in the current model [70, 71]. Phagocytosis, measured by bead uptake in isolated microglia, decreased with dexamethasone recovery (Fig 8(Ai)), yet when measuring mean uptake per cell (Fig 8(Aii)) phagocytosis remained broadly elevated in the dexamethasone recovery groups. Similarly, myelin phagocytosis in mixed glial cultures is altered by dexamethasone recovery treatment, decreasing in percent phagocytes but remaining elevated in uptake per cell in the LPS/IFN condition. This may be indicative of a *primed* microglia phenotype as described in relation to myelin degradation in multiple sclerosis, myelin dysregulation in early onset dementia, or the loss of oligodendroglia progenitors and myelin in cerebral palsy [18, 72–74]. Alternately, as our analysis is based on internalization of endogenous oligodendrocyte markers, this assay may be confounded by changes in the turnover of oligodendrocytes in vitro, which would necessitate increased clearance in the case of higher oligodendrocyte death. Altogether, different degrees of *priming* in microglia may be approximated by this model. Dexamethasone may be the most representative, especially in isolated microglia, due to the incomplete *surveying* restoration in the expression of NO, TNF, IL-1β, NGF, CD68, and MHCII, partially ramified morphology, and alteration in phagocytosis.

Summary and Conclusion

Ramified *surveying*, *activated*, and *primed* microglial phenotypes were acutely recreated in vitro with potent pro- and anti-inflammatory treatments. Microglia, from an isolated and mixed glial cultures including astrocytes and oligodendrocytes, were treated for 6 h with LPS. Anti-inflammation was modeled with 18-h treatments with dexamethasone. The cells were then treated for 24 h with interferon gamma (IFNγ) to detect inflammatory memory after recovery. Nitric oxide (NO), cytokines (TNF, IL-1β, IL-10), and growth factor (BDNF, GDNF, NGF) secretions, microglial morphology and labels (iNOS, CD68, MHCII), proliferation (EdU), and phagocytosis (microbead and myelin via CNPase) were characterized. This spectrum of cellular presentation and behavior was measured to assess the expected phenotypes.

A *surveying* phenotype was best represented in the untreated Veh case and was characterized by a basal or reduced expression of pro-inflammatory cytokines, NO, iNOS, MHCII, proliferation, and phagocytosis. Additionally, this was accompanied by higher BDNF and GDNF production and smaller microglia with thin branching processes. *Activation* was observed predominantly the LPS and LPS/IFNγ treatment groups. This was followed by an increase in cytokines, NO, NGF, iNOS, proliferation, phagocytosis, and a reduction in BDNF. Morphology was depicted by a flattened round amoeboid shape. Degrees of microglial *priming* were noted in dexamethasone when comparing LPS, IFNγ, and LPS/IFNγ with each other observing incomplete *surveying* restoration from *activation*. As such, dexamethasone resulted in a profound dysregulation of NO, TNF, IL-1β, NGF, CD68, and MHCII expression, as well as restored ramified morphology and inflammation-mediated myelin endocytosis that was sustained after washout of dexamethasone.

Materials and Methods

Materials

Dulbecco's modified Eagle medium: Nutrient Mixture F12 (DMEM F12), Hank's Balanced Salt Solution (HBSS), fetal bovine serum (FBS), penicillin streptomycin (PS), 0.25% trypsin-ethylenediaminetetraacetic acid (Trypsin-EDTA), and normal horse serum (NHS) were purchased from Gibco (Life Technologies, Burlington, ON, Canada). Poly-L-lysine hydrobromide (PLL), dexamethasone, polyethylene glycol 300 (PEG300), and lipopolysaccharide (LPS) were purchased from Sigma Aldrich (St. Louis, MO, USA). Interferon gamma was purchased from Peprotech (Montreal, QC, Canada). Polystyrene 75 cm^3 flasks were purchased from Corning (Corning, NY, USA). Polystyrene 12-well cell culture plates were purchased from Greiner Bio-One (Frickenhausen, Germany).

The following primary antibodies were used: mouse anti-iNOS (Santa Cruz Biotechnology, Santa Cruz, CA, USA), mouse anti-CD68 (BioRad, Burlington, ON, Canada), mouse anti-MHCII (Abcam, Toronto, ON, Canada), mouse anti-CD11b (Millipore, Etobicoke, ON, Canada), rabbit anti-BDNF (Abcam), rabbit anti-GDNF (Abcam), rabbit anti-NGF (Abcam), rabbit anti-Iba1 (Wako, Osaka, Japan), chicken anti-GFAP (Abcam), and mouse anti-CNPase (Abcam).

The following secondary antibodies were used: donkey anti-mouse Alexa Fluor 488 (Invitrogen, Burlington, ON, Canada), goat anti-chicken Alexa Fluor 546 (Invitrogen), donkey anti-mouse Alexa Fluor 647 (Invitrogen), donkey anti-rabbit Alexa Fluor 647 (Invitrogen), and donkey anti-rabbit IR Dye 680RD (Li-Cor, Lincoln, NE, USA). Hoescht 33342 was purchased from Molecular Probes (Life Technologies, Burlington, ON, Canada). Fluoromount-G was purchased from Southern Biotech (Birmingham, AL, USA).

Primary Microglial Cell Culture and Treatments

Animal protocols were approved by the Animal Care and Use Committee at the University of Alberta and conducted in accordance with animal ethics guidelines. Mixed glial cells (microglia, astrocytes, oligodendrocytes) were harvested from postnatal day 1 male Sprague-Dawley rats [75]. The rats were decapitated and their brains removed with the aid of surgical scissors and a metal spatula. While in HBSS with 1% PS, the brains were removed of their meninges and vasculature and dissociated in 0.25% Trypsin-EDTA (2 mL/brain) at 37 °C for 25 min. Following two-fold centrifugation at 500 g for 2 min and trituration in culturing media (DMEM F12/10% FBS/1% PS) in order to further dissociate the brain tissue and deactivate any residual Trypsin-EDTA, the resulting cell suspension was placed in 75 cm^2 flasks coated with PLL (2 μg/mL). Cells were incubated for 2 weeks at 37 °C and 5% CO_2, with culturing media changed twice weekly. Confluency was achieved after a culture period of 14 days in vitro.

To acquire microglial cell cultures, confluent cell layers were washed with DMEM F12 and then lifted off from the 12-well plates with a 0.25% Trypsin-EDTA and DMEM F12 mixture (1:3) treatment for 20 min [76]. Mixed glial cells were collected and subjected to two-fold centrifugation at 500 *g* for 2 min and trituration in culturing media, and were deposited onto 12-well plates coated with PLL (2 μg/mL). Isolated microglial cultures were cultured in DMEM F12/1% FBS/1% PS media.

The timeline and experimental design are as follows: the cells were activated with LPS (100 ng/mL) for 6 h (*hyper-activated*) and recovered 18 h (*primed*) with an effective anti-inflammatory treatment dexamethasone (Dex, 10 μM). To fully suspend the treatments, the vehicle (Veh) contained 0.5% PEG300 in DMEM F12, which was included in dexamethasone as a final working concentration. These cells were afterwards treated with IFNγ (100 ng/mL) for 24 h to detect whether cells were primed by their previous activation.

Immunocytochemistry and In-Cell Western Assays

Cell cultures were fixed with 5% formalin at 37 °C for 10 min and washed once with phosphate-buffered saline (PBS). Cells were then permeabilized with 0.1% Triton X-100 (TX100) in PBS and 10% Normal Horse Serum (NHS) for 1 h. Following this, the cells were incubated overnight at 4 °C in PBS with one of the following primary antibodies plus 1% NHS: mouse anti-iNOS (1:1000), mouse anti-CD68 (1:500), mouse anti-MHCII (1:500), mouse anti-CD11b (1:500), rabbit anti-BDNF (1:500), rabbit anti-GDNF (1:500), rabbit anti-NGF (1:250), rabbit anti-Iba1 (1:1000), chicken anti-GFAP (1:5000), and mouse anti-CNPase (1:1000). Primary antibodies were then aspirated and washed three times with PBS, followed by incubation for 1 h at room temperature in PBS with one of the following secondary antibodies plus 1% NHS and Hoescht 33342 (1:1000): For Iba1/GFAP/CNPase, donkey anti-mouse Alexa Fluor 488 (1:200), goat anti-chicken Alexa Fluor 546 (1:200), and donkey anti-rabbit Alexa Fluor 647 (1:200) were used. For iNOS/CD68/MHCII, donkey anti-mouse Alex Fluor 647 (1:500) was used. For BDNF/GDNF/NGF, donkey anti-rabbit Alexa Fluor 647 (1:500) was used.

Coverslips were placed into the wells of plates and imaged on a Leica DMI6000B inverted fluorescent microscope (Leica Microsystems, Wetzlar, Germany). For high-resolution imaging, cells were cultured on PLL-coated glass coverslips which were fixed and subjected to immunocytochemistry as described above. Following immunocytochemistry, coverslips were inverted onto Fluoromount-coated glass slides and imaged on a Leica TCS SPE inverted confocal microscope (Leica Microsystems).

For in-cell Western assays, an Odyssey CLx infrared imaging system (Li-Cor) was used to scan cell cultures in 48-well plates. Whole plates were scanned and wells were compared with regard to relative intensity. Specimens were immunolabeled for BDNF, GDNF, and NGF according to the protocol described above but incubated with donkey anti-rabbit IR Dye 680RD (1:4000).

Molecular Analyses

Levels of the nitrite metabolite of nitric oxide (NO) were measured via the Griess reaction [77]. Enzyme-linked immunosorbent assays (ELISA) for TNF, IL-1β, and IL-10 were performed according to the manufacturer's instructions, with modifications (R&D Systems, Minneapolis, MN). Briefly, 96-well plates were coated with the appropriate capture antibody in PBS overnight at room temperature. Plates were blocked with 1% bovine serum albumin (BSA) in PBS for 1 h at room temperature, following which samples or standards were added and incubated overnight at 4 °C. Adhering antigen was detected by sequential incubation with the respective biotin-conjugated detection antibody for 1 h followed by horseradish peroxidase-conjugated streptavidin for 20 min (each in PBS + 1% BSA). All preceding steps were separated by 3× washing phases with PBS + 0.05% Tween-20 (PBS-T).

Fluorescence was developed by addition of 100 μM 10-acetyl-3,7-dihydroxyphenoxazine (Amplex Red) and 0.3% H_2O_2 in PBS for 20 min at room temperature. Fluorescence was measured at an excitation wavelength of 540 nm and emission wavelength of 590 nm (SpectraMax M3, Molecular Devices).

Cell Proliferation Assay

Proliferation was measured by the incorporation of the synthetic nucleotide 5-ethynyl-2′-deoxyuridine (EdU), and visualized using the Click-iT® EdU Alexa Fluor® 555 Imaging Kit (Life Technologies) according to manufacturer's protocol with modifications (Koss et al. 2016; Krishan and Hamelik, 2010; Mead and Lefebvre 2014). In brief, live cells were incubated with 10 μM EdU for 24 h at 37 °C, 5% CO_2, and subsequently fixed and permeabilized as above. Fixed cells were then incubated for 30 min at 37 °C in 100 mM Tris buffer (pH 8.5) containing 50 mM ascorbic acid, 10 mM CuSO4, and 10 μM Alexa Fluor 555 azide. After three washings in PBS (pH 7.4), immunolabeling for Iba-1 and nuclear counterstaining with Hoechst 33342 was performed as outlined above. Basic images were taken using confocal microscopy.

Cell Phagocytosis Assay

Phagocytosis was measured by treating cells with 10 μm green fluorescent polystyrene beads (Sigma Aldrich). Beads were diluted 1:1000 into working solutions of DMEM F12 and cells were treated (1 mL per well) for 2 h prior to fixation. Immunolabeling with iNOS, CD68, MHCII, and nuclear counterstaining with Hoechst 33342 was performed as outlined above. Basic images were taken using confocal microscopy.

Image and Statistical Analyses

For quantification of labels, images were systematically acquired using epifluorescence microscopy on a 4 × 5 grid, resulting in 20 images per condition to eliminate acquisition bias. Images were quantified by automated analysis using custom written macros in ImageJ.

Overall significance was assessed using two-way analyses of variance, with a Bonferroni multiple comparison post-hoc analysis between groups. A p value of ≤ 0.05 was considered significant. Where * and † represent comparisons within (pairwise) and across (group-wise) Veh and dexamethasone groups, respectively. Each reported n indicates an independent experiment from a separate culture preparation.

Acknowledgements The authors would like to acknowledge Lexis Galarneau, Stephan Tchir, Yawa Idi, and Patricia Kent for their assistance with laboratory work and conceptualization. The authors are also grateful for financial support from the Canada Foundation for Innovation, Alberta Health Services, and the Davey Endowment for Brain Research.

Publisher's Note Springer Nature remains neutral with regard to jurisdictional claims in published maps and institutional affiliations.

References

1. Aarli JA, Dua T, Aleksandar J, Muscetta A (2006) Neurological disorders public health challenges. In: World Health Organ. http://www.who.int/mental_health/neurology/neurological_disorders_report_web.pdf. Accessed 13 Jan 2018
2. Wong SL, Gilmour H, Ramage-Morin PL (2014) Parkinson's disease: prevalence, diagnosis and impact. Health Rep 25:10–14
3. Wong SL, Gilmour H, Ramage-Morin PL (2016) Alzheimer's disease and other dementias in Canada. Health Rep 27:11–16
4. Prinz M, Priller J (2014) Microglia and brain macrophages in the molecular age: from origin to neuropsychiatric disease. Nat Rev Neurosci 15:300–312. https://doi.org/10.1038/nrn3722
5. Ransohoff RM (2016) How neuroinflammation contributes to neurodegeneration. Science 353:777–783. https://doi.org/10.1126/science.aag2590
6. Buchman AL (2001) Side effects of corticosteroid therapy. J Clin Gastroenterol 33:289–294
7. Sun W-H, He F, Zhang N-N, Zhao ZA, Chen HS (2018) Time dependent neuroprotection of dexamethasone in experimental focal cerebral ischemia: the involvement of NF-κB pathways. Brain Res 1701:237–245. https://doi.org/10.1016/j.brainres.2018.09.029
8. Feng Y, Lu S, Wang J, Kumar P, Zhang L, Bhatt AJ (2014) Dexamethasone-induced neuroprotection in hypoxic-ischemic brain injury in newborn rats is partly mediated via Akt activation. Brain Res 1589:68–77. https://doi.org/10.1016/j.brainres.2014.09.073
9. Rangarajan P, Eng-Ang L, Dheen ST (2013) Potential drugs targeting microglia: current knowledge and future prospects. CNS Neurol. Disord.-Drug Targets 12:799–806
10. Baby N, Patnala R, Ling E-A, Dheen ST (2014) Nanomedicine and its application in treatment of microglia-mediated neuroinflammation. Curr Med Chem 21:4215–4226
11. Brown RJ, Rother KI, Artman H, Mercurio MG, Wang R, Looney RJ, Cowen EW (2009) Minocycline-induced drug hypersensitivity syndrome followed by multiple autoimmune sequelae. Arch Dermatol 145:63–66. https://doi.org/10.1001/archdermatol.2008.521
12. Medzhitov R (2008) Origin and physiological roles of inflammation. Nature 454:428–435. https://doi.org/10.1038/nature07201
13. Banks WA (2016) From blood-brain barrier to blood-brain interface: new opportunities for CNS drug delivery. Nat Rev Drug Discov 15:275–292. https://doi.org/10.1038/nrd.2015.21
14. Lehnardt S (2010) Innate immunity and neuroinflammation in the CNS: the role of microglia in toll-like receptor-mediated neuronal injury. Glia 58:253–263. https://doi.org/10.1002/glia.20928
15. Ransohoff RM (2016) A polarizing question: do M1 and M2 microglia exist? Nat Neurosci 19:987–991. https://doi.org/10.1038/nn.4338
16. Tang Y, Le W (2016) Differential roles of M1 and M2 microglia in neurodegenerative diseases. Mol Neurobiol 53:1181–1194. https://doi.org/10.1007/s12035-014-9070-5
17. Witcher KG, Eiferman DS, Godbout JP (2015) Priming the inflammatory pump of the CNS after traumatic brain injury. Trends Neurosci 38:609–620. https://doi.org/10.1016/j.tins.2015.08.002
18. Harry GJ, Kraft AD (2012) Microglia in the developing brain: a potential target with lifetime effects. Neurotoxicology 33:191–206. https://doi.org/10.1016/j.neuro.2012.01.012

19. Lobo-Silva D, Carriche GM, Castro AG, Roque S, Saraiva M (2016) Balancing the immune response in the brain: IL-10 and its regulation. J Neuroinflammation 13:297. https://doi.org/10.1186/s12974-016-0763-8
20. Gravel M, Béland L-C, Soucy G et al (2016) IL-10 controls early microglial phenotypes and disease onset in ALS caused by misfolded superoxide dismutase 1. J Neurosci 36:1031–1048. https://doi.org/10.1523/JNEUROSCI.0854-15.2016
21. Park KW, Lee HG, Jin BK, Lee YB (2007) Interleukin-10 endogenously expressed in microglia prevents lipopolysaccharide-induced neurodegeneration in the rat cerebral cortex in vivo. Exp Mol Med 39:812–819. https://doi.org/10.1038/emm.2007.88
22. Sierra A, Beccari S, Diaz-Aparicio I, Encinas JM, Comeau S, Tremblay MÈ (2014) Surveillance, phagocytosis, and inflammation: how never-resting microglia influence adult hippocampal neurogenesis. Neural Plast 2014:610343. https://doi.org/10.1155/2014/610343
23. Nakajima K, Kohsaka S (2001) Microglia: activation and their significance in the central nervous system. J Biochem 130:169–175
24. Lull ME, Block ML (2010) Microglial activation and chronic neurodegeneration. Neurother 7:354–365. https://doi.org/10.1016/j.nurt.2010.05.014
25. von Bernhardi R, Eugenín-von Bernhardi L, Eugenín J (2015) Microglial cell dysregulation in brain aging and neurodegeneration. Front Aging Neurosci 7:. https://doi.org/10.3389/fnagi.2015.00124
26. Norden DM, Godbout JP (2013) Microglia of the aged brain: primed to be activated and resistant to regulation. Neuropathol Appl Neurobiol 39:19–34. https://doi.org/10.1111/j.1365-2990.2012.01306.x
27. Perry VH, Holmes C (2014) Microglial priming in neurodegenerative disease. Nat Rev Neurol 10:217–224. https://doi.org/10.1038/nrneurol.2014.38
28. Hennessy E, Griffin ÉW, Cunningham C (2015) Astrocytes are primed by chronic neurodegeneration to produce exaggerated chemokine and cell infiltration responses to acute stimulation with the cytokines IL-1β and TNF-α. J Neurosci 35:8411–8422. https://doi.org/10.1523/JNEUROSCI.2745-14.2015
29. Holtman IR, Raj DD, Miller JA, Schaafsma W, Yin Z, Brouwer N, Wes PD, Möller T et al (2015) Induction of a common microglia gene expression signature by aging and neurodegenerative conditions: a co-expression meta-analysis. Acta Neuropathol Com 3:31. https://doi.org/10.1186/s40478-015-0203-5
30. Norden DM, Muccigrosso MM, Godbout JP (2015) Microglial priming and enhanced reactivity to secondary insult in aging, and traumatic CNS injury, and neurodegenerative disease. Neuropharmacology 96:29–41. https://doi.org/10.1016/j.neuropharm.2014.10.028
31. Cregg JM, DePaul MA, Filous AR et al (2014) Functional regeneration beyond the glial scar. Exp Neurol 253:197–207. https://doi.org/10.1016/j.expneurol.2013.12.024
32. Okada S, Hara M, Kobayakawa K, Matsumoto Y, Nakashima Y (2018) Astrocyte reactivity and astrogliosis after spinal cord injury. Neurosci Res 126:39–43. https://doi.org/10.1016/j.neures.2017.10.004
33. Raposo C, Schwartz M (2014) Glial scar and immune cell involvement in tissue remodeling and repair following acute CNS injuries. Glia 62:1895–1904. https://doi.org/10.1002/glia.22676
34. Avignone E, Lepleux M, Angibaud J, Nägerl UV (2015) Altered morphological dynamics of activated microglia after induction of status epilepticus. J Neuroinflammation 12:202. https://doi.org/10.1186/s12974-015-0421-6
35. Lee Y, Lee S-R, Choi SS, Yeo HG, Chang KT, Lee HJ (2014) Therapeutically targeting neuroinflammation and microglia after acute ischemic stroke. Biomed Res Int 2014:297241. https://doi.org/10.1155/2014/297241
36. Heneka MT, Sastre M, Dumitrescu-Ozimek L, Dewachter I, Walter J, Klockgether T, van Leuven F (2005) Focal glial activation coincides with increased BACE1 activation and precedes amyloid plaque deposition in APP [V717I] transgenic mice. J Neuroinflammation 2:22. https://doi.org/10.1186/1742-2094-2-22
37. Solito E, Sastre M (2012) Microglia function in Alzheimer's disease. Front Pharmacol 3:14. https://doi.org/10.3389/fphar.2012.00014
38. Wyss-Coray T, Rogers J (2012) Inflammation in Alzheimer disease—a brief review of the basic science and clinical literature. CSH Perspect Med 2:a006346. https://doi.org/10.1101/cshperspect.a006346
39. Mandrekar-Colucci S, Landreth GE (2010) Microglia and inflammation in Alzheimer's disease. CNS Neurol Disord Drug Targets 9:156–167
40. Qian L, Flood PM (2008) Microglial cells and Parkinson's disease. Immunol Res 41:155–164. https://doi.org/10.1007/s12026-008-8018-0
41. Jack C, Ruffini F, Bar-Or A, Antel JP (2005) Microglia and multiple sclerosis. J Neurosci Res 81:363–373. https://doi.org/10.1002/jnr.20482
42. Compston A, Coles A (2008) Multiple sclerosis. Lancet 372:1502–1517. https://doi.org/10.1016/S0140-6736(08)61620-7
43. Dheen ST, Kaur C, Ling E-A (2007) Microglial activation and its implications in the brain diseases. Curr Med Chem 14:1189–1197
44. Chen Z, Jalabi W, Shpargel KB, Farabaugh KT, Dutta R, Yin X, Kidd GJ, Bergmann CC et al (2012) Lipopolysaccharide-induced microglial activation and neuroprotection against experimental brain injury is independent of Hematogenous TLR4. J Neurosci 32:11706–11715. https://doi.org/10.1523/JNEUROSCI.0730-12.2012
45. Takeuchi H, Wang J, Kawanokuchi J, Mitsuma N, Mizuno T, Suzumura A (2006) Interferon-gamma induces microglial-activation-induced cell death: a hypothetical mechanism of relapse and remission in multiple sclerosis. Neurobiol Dis 22:33–39. https://doi.org/10.1016/j.nbd.2005.09.014
46. Ling EA, Wong WC (1993) The origin and nature of ramified and amoeboid microglia: a historical review and current concepts. Glia 7:9–18. https://doi.org/10.1002/glia.440070105
47. Rock RB, Gekker G, Hu S, Sheng WS, Cheeran M, Lokensgard JR, Peterson PK (2004) Role of microglia in central nervous system infections. Clin Microbiol Rev 17:942–964. https://doi.org/10.1128/CMR.17.4.942-964.2004
48. Glenn JA, Ward SA, Stone CR et al (1992) Characterisation of ramified microglial cells: detailed morphology, morphological plasticity and proliferative capability. J Anat 180:109–118
49. Boche D, Perry VH, Nicoll JA (2013) Review: activation patterns of microglia and their identification in the human brain. Neuropathol Appl Neurobiol 39:3–18. https://doi.org/10.1111/nan.12011
50. Nayak D, Roth TL, McGavern DB (2014) Microglia development and function. Annu Rev Immunol 32:367–402. https://doi.org/10.1146/annurev-immunol-032713-120240
51. Lan X, Han X, Li Q, Yang QW, Wang J (2017) Modulators of microglial activation and polarization after intracerebral haemorrhage. Nat Rev Neurol 13:420–433. https://doi.org/10.1038/nrneurol.2017.69
52. Heese K, Fiebich BL, Bauer J, Otten U (1998) NF-kappaB modulates lipopolysaccharide-induced microglial nerve growth factor expression. Glia 22:401–407
53. Plane JM, Shen Y, Pleasure DE, Deng W (2010) Prospects for minocycline neuroprotection. Arch Neurol 67:1442–1448. https://doi.org/10.1001/archneurol.2010.191
54. Elewa HF, Hilali H, Hess DC, Machado LS, Fagan SC (2006) Minocycline for acute neuroprotection. Pharmacotherapy 26:515–521. https://doi.org/10.1592/phco.26.4.515

55. Bélanger M, Magistretti PJ (2009) The role of astroglia in neuroprotection. Dialogues Clin Neurosci 11:281–295
56. Liu Z, Chopp M (2016) Astrocytes, therapeutic targets for neuroprotection and neurorestoration in ischemic stroke. Prog Neurobiol 144:103–120. https://doi.org/10.1016/j.pneurobio.2015.09.008
57. Lively S, Schlichter LC (2013) The microglial activation state regulates migration and roles of matrix-dissolving enzymes for invasion. J Neuroinflammation 10(75). https://doi.org/10.1186/1742-2094-10-75
58. Hines DJ, Choi HB, Hines RM, Phillips AG, MacVicar BA (2013) Prevention of LPS-induced microglia activation, cytokine production and sickness behavior with TLR4 receptor interfering peptides. PLoS One 8:e60388. https://doi.org/10.1371/journal.pone.0060388
59. Nimmervoll B, White R, Yang J-W, An S, Henn C, Sun JJ, Luhmann HJ (2013) LPS-induced microglial secretion of TNFα increases activity-dependent neuronal apoptosis in the neonatal cerebral cortex. Cereb Cortex 23:1742–1755. https://doi.org/10.1093/cercor/bhs156
60. Tam WY, Au NPB, Ma CHE (2016) The association between laminin and microglial morphology *in vitro*. Sci Rep 6:28580. https://doi.org/10.1038/srep28580
61. Gomes C, Ferreira R, George J, Sanches R, Rodrigues DI, Gonçalves N, Cunha RA (2013) Activation of microglial cells triggers a release of brain-derived neurotrophic factor (BDNF) inducing their proliferation in an adenosine A2A receptor-dependent manner: A2A receptor blockade prevents BDNF release and proliferation of microglia. J Neuroinflammation 10:780. https://doi.org/10.1186/1742-2094-10-16
62. Walker DG, Lue L-F (2015) Immune phenotypes of microglia in human neurodegenerative disease: challenges to detecting microglial polarization in human brains. Alzheimers Res Ther 7:56. https://doi.org/10.1186/s13195-015-0139-9
63. Harms AS, Cao S, Rowse AL, Thome AD, Li X, Mangieri LR, Cron RQ, Shacka JJ et al (2013) MHCII is required for α-synuclein-induced activation of microglia, CD4 T cell proliferation, and dopaminergic neurodegeneration. J Neurosci 33:9592–9600. https://doi.org/10.1523/JNEUROSCI.5610-12.2013
64. Pascual O, Achour SB, Rostaing P et al (2012) Microglia activation triggers astrocyte-mediated modulation of excitatory neurotransmission. Proc Natl Acad Sci 109:E197–E205. https://doi.org/10.1073/pnas.1111098109
65. Shinozaki Y, Nomura M, Iwatsuki K, Moriyama Y, Gachet C, Koizumi S (2014) Microglia trigger astrocyte-mediated neuroprotection via purinergic gliotransmission. Sci Rep 4:4329. https://doi.org/10.1038/srep04329
66. Niraula A, Sheridan JF, Godbout JP (2017) Microglia priming with aging and stress. Neuropsychopharmacology 42:318–333. https://doi.org/10.1038/npp.2016.185
67. Murray M, Fischer I (2001) Transplantation and gene therapy: combined approaches for repair of spinal cord injury. Neuroscientist 7:28–41. https://doi.org/10.1177/107385840100700107
68. Nakajima K, Honda S, Tohyama Y, Imai Y, Kohsaka S, Kurihara T (2001) Neurotrophin secretion from cultured microglia. J Neurosci Res 65:322–331. https://doi.org/10.1002/jnr.1157
69. Rizzi C, Tiberi A, Giustizieri M, et al NGF steers microglia toward a neuroprotective phenotype. Glia 0: https://doi.org/10.1002/glia.23312, 2018
70. Hanisch U-K, Kettenmann H (2007) Microglia: active sensor and versatile effector cells in the normal and pathologic brain. Nat Neurosci 10:1387–1394. https://doi.org/10.1038/nn1997
71. Ransohoff RM, Perry VH (2009) Microglial physiology: unique stimuli, specialized responses. Annu Rev Immunol 27:119–145. https://doi.org/10.1146/annurev.immunol.021908.132528
72. Domingues HS, Portugal CC, Socodato R, Relvas JB (2016) Oligodendrocyte, astrocyte, and microglia crosstalk in myelin development, damage, and repair. Front Cell Dev Biol 4:. https://doi.org/10.3389/fcell.2016.00071
73. Klünemann HH, Ridha BH, Magy L et al (2005) The genetic causes of basal ganglia calcification, dementia, and bone cysts: DAP12 and TREM2. Neurology 64:1502–1507. https://doi.org/10.1212/01.WNL.0000160304.00003.CA
74. Deng W, Pleasure J, Pleasure D (2008) Progress in periventricular leukomalacia. Arch Neurol 65:1291–1295. https://doi.org/10.1001/archneur.65.10.1291
75. Chen S-H, Oyarzabal EA, Hong J-S (2013) Preparation of rodent primary cultures for neuron–glia, mixed glia, enriched microglia, and reconstituted cultures with microglia. In: Joseph B, Venero JL (eds) Microglia: Methods and protocols. Humana Press, Totowa, pp. 231–240
76. Churchward MA, Todd KG (2014) Statin treatment affects cytokine release and phagocytic activity in primary cultured microglia through two separable mechanisms. Mol Brain 7:1–12. https://doi.org/10.1186/s13041-014-0085-7
77. Griess P (1879) Bemerkungen zu der Abhandlung der HH. Weselsky und Benedikt "Ueber einige Azoverbindungen." Berichte Dtsch Chem Ges. https://doi.org/10.1002/cber.187901201117